AN UPGRADED EXTRACTION SEPTUM AND A NEW DIAGNOSTIC SECTION FOR THE BONN ISOCHRONOUS CYCLOTRON

D. Sauerland*, S. Neubert, University of Bonn, Bonn, Germany

Abstract

The Bonn Isochronous Cyclotron provides light ion beams of a charge-to-mass ratio $Q/A \geq 1/2$ with kinetic energies ranging from 7 MeV to 14 MeV/A to five experimental sites. To improve operation reliability, the cyclotron's electrostatic extraction septum is upgraded using components, manufactured by laser-powder bed fusion (L-PBF). The new copper septum blade holder reduces thermal load on the blade and the integrated cooling system's leak rates to the vacuum. Also, a new beam diagnostic section for the future ion beam analysis setup in Beamline D is under construction, comprising a secondary electron monitor, a Faraday cup (FC) and a beam screen (BS). Both, FC and BS, are made from aluminium using L-PBF and are pneumatically retractable. Cooling is provided through coaxial water tubes, integrated into the pneumatic rods. Here, progress of the septum upgrade will be reported and details of the new diagnostic section will be provided.

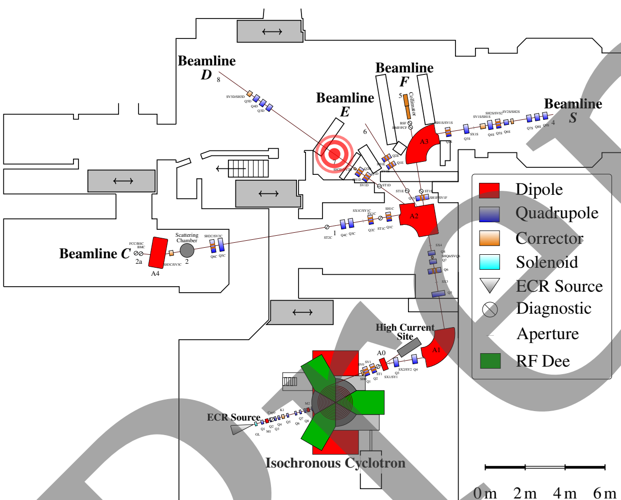

Figure 1: Overview of the accelerator facility with future location of the diagnostic section.

BONN ISOCHRONOUS CYCLOTRON

Figure 1 shows the accelerator facility of the Bonn Isochronous Cyclotron. The cyclotron supplies five experimental sites with proton, deuteron, alpha and other light ion beams of $Q/A \geq 1/2$ at kinetic energies between 7 and 14 MeV/A. 14 MeV protons are used at the high-homogeneity irradiation site. 28 MeV Deuterons are utilized to generate a neutron beam, using a copper/tungsten collimator. This beamline is currently being commissioned. In future, low energetic alphas will be used in an ion beam analysis setup (IBA), comprising Rutherford backscattering and particle-induced X-ray emission.

The ion beam is provided by two external electron cyclotron resonance (ECR) sources located beside and underneath the cyclotron. The generated 2 to 8 keV ions are transported through the low-energy beam line and are injected axially into the cyclotron's magnetic center using an electrostatic hyperboloid inflector.

The Bonn Isochronous Cyclotron [1] is designed as a three-sector isochronous AVF cyclotron featuring a magnetic field distribution with 120° rotational symmetry. For this purpose, the magnet structure is subdivided into three hill and three valley regions without spiral shaping. Each valley accommodates a broadband dual-gap dee resonator capable of providing peak acceleration voltages of up to 40 kV. Routine operation is performed at the third harmonic, where the applied RF frequency amounts to three times the ions' orbital frequency. Accessible Q/A is constrained by the RF frequency range and the maximum average magnetic flux density.

After about 120 turns, the beam is extracted by an electrostatic septum into a field-compensated extraction channel. The extracted particles are subsequently transported either to the high-current site or via the high-energy beam line to five experimental areas.

EXTRACTION SEPTUM UPGRADE

The main component in the cyclotron's extraction is the septum. Once the beam passes a 0.2 mm-thick tungsten septum blade, it is deflected into the extraction channel by static electric fields between blade and antiseptum, biased with up to 40 kV.

As already discussed in Ref. [2], a septum upgrade is in progress. The upgrade includes a redesigned antiseptum with improved operation reliability and a newly developed copper blade holder with integrated water cooling, manufactured utilizing the laser-powder bed fusion technique (L-PBF). Thermal simulations, using `CST Studio`, indicated an enhanced cooling performance and reduced thermal load on the septum blade compared to the previous design.

Testing a First Prototype

One prototype blade holder has been manufactured for test purposes. After copper tubes have been soldered to the cooling channel's in- and outlet, its leak rate has been measured as $6.2(3) \times 10^{-9}$ mbar l s^{-1}, using a helium leak detector. Additionally, the holder with air-filled cooling channel has been integrated into a vacuum recipient and repeatedly evacuated with a turbo molecular pump.

As is shown in Fig. 2, no systematic differences in the pressure evolution during evacuation were observed between

* sauerland@hiskp.uni-bonn.de

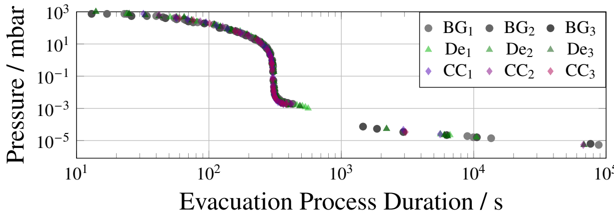

Figure 2: Vacuum recipient pressure during three evacuation processes i.

measurements without the holder (BG_i), with inserted holder (De_i), or with the holder's cooling channel also being connected to atmosphere (CC_i). Thus, neither enhanced desorption from the L-PBF manufactured component nor leaks from the cooling channel into the vacuum system could be identified. Although, the desired vacuum pressure could be reached, the holder's torsional stiffness and its needed installation space into the septum with soldered tubes were insufficient, necessitating an update to the holder's design.

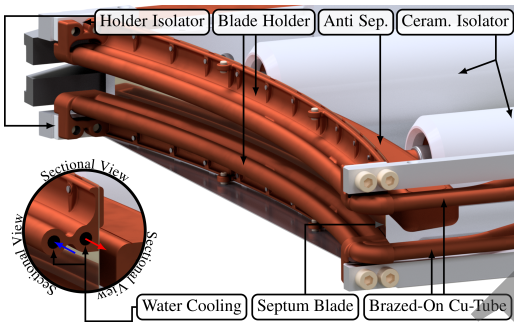

Figure 3: CAD rendering of the extraction septum with an updated blade holder design and sectional view of its integrated water cooling channel.

Update of the Blade Holder Design

A CAD rendering of the installed blade holder in an updated design is shown in Fig. 3. The holder shows an increased torsional stiffness due to an enforced distal edge. It has been manufactured twice and is currently being tested. Here, the return line of the cooling channel has been extended close to its inlet, allowing two tubes to be soldered side by side at the in- and outlet, thereby reducing the required radial installation space. Measured leak rates of $< 10^{-12}$ mbar l s^{-1} of one unit's cooling channel and $2(1) \times 10^{-12}$ mbar l s^{-1} of the other[1], indicate a reduced permeation of gases through the cooling channel's wall, as its thickness has been increased from 1 to 2 mm. After identifying and mitigating the cause of the units' initial leak rate differences, additional holders will be ordered and the upgrade of the three septa will be carried out.

NEW DIAGNOSTIC SECTION

At the start of each of the facility's five beamlines, a dedicated diagnostic section should provide information about the beam's current, its position and transversal profile. For this purpose, a new diagnostic section has been designed and will be first installed in Beamline D for the future IBA setup (comp. Fig. 1, red dot).

The section comprises a secondary electron monitor (SEM), a Faraday cup (FC) and a beam screen (BS) (see Fig. 4, right). FC and BS can be pneumatically inserted into the beam path; when retracted, the beam passes only through the SEM, not constricting the beam path. The diagnostics' mounting plate is connected to the support frame below via a three-point suspension system, allowing for its precise positioning using a laser tracker. To maintain a vacuum pressure $< 10^{-6}$ mbar during operation, a turbo molecular pump is installed in the frame, too.

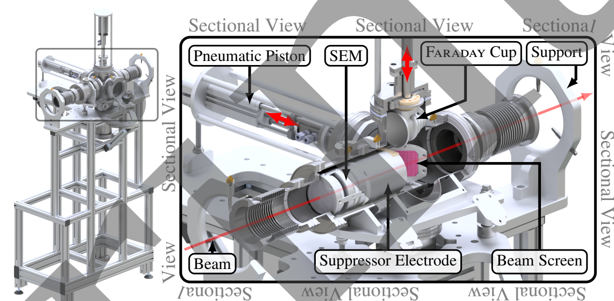

Figure 4: CAD rendering of the complete diagnostics section (left), featuring an enlarged cross-sectional view of the individual diagnostics modules (right).

Secondary Electron Monitor and Faraday Cup

The SEM, based on Ref. [3], uses the surface emission of secondary electrons (SE) upon impact of fast ions into matter, to non-destructively measure the beam's current and relative position. It consists of two pairs of electrically isolated horizontally (SEM U & D) and vertically (SEM L & R) segmented 0.8 µm-thick Al foils. Emitted SE are removed by three pull electrodes, which are 0.8 µm-thick Al foils located in close proximity to the SEM foils and biased at +150 V. The SEM foils' total current is proportional to the beam current whereas foil-segmentation allows for a relative position measurement.

`CST Studio` is used to simulate SE emission and propagation in the electrostatic fields of the SEM and also includes SE-generated space charge effects. A scenario with a 13.6 MeV proton beam with 1 µA current is shown in Fig. 5. Proton-induced SE yield (SEY) is based on Ref. [4], including an up- to downstream SEY-asymmetry [5]. The SE's emission energy probability density function is assumed as a gamma distribution with mean energy of 15 eV [6]. In the simulated SEM design, the average SE collection efficiency is 97.3(5) % at +150 V pull electrode voltage.

For SEM-calibration and direct beam current measurements, an FC is located downstream of the SEM. Its inverted cone-shape prevents an escape of most SE, as their emission probability distribution is maximal at an angle parallel to the surface normal. For SE with unfavorable emission angles, an upstream cylindrical suppressor electrode, biased with

[1] Initial leak rates of $> 10^{-3}$ mbar l s^{-1} due to manufacturing issues have been mitigated, using low-viscosity anaerobic adhesive.

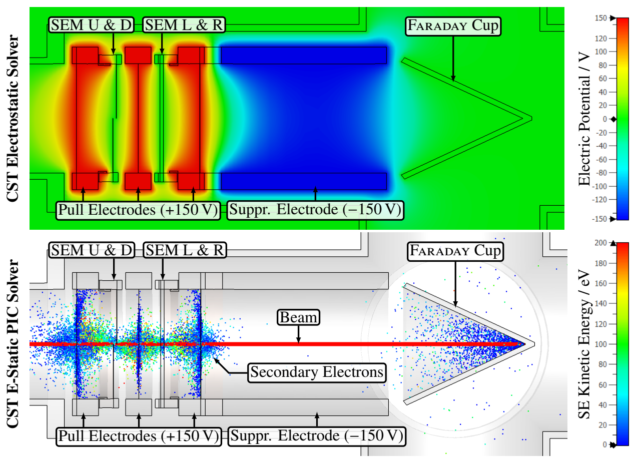

Figure 5: Simulated electric potential of SEM and FC (top) and spatial distribution of SE for a proton beam current of 1 µA in its equilibrium state (bottom).

−150 V, repels them back into the cup. In the above scenario, the FC has a charge collection efficiency of 99.96(5) %.

To dissipate the incident beam's heat load, the L-PBF-manufactured FC from Al features 6 mm-diameter cooling channels for ultrapure water, spiraling along its surface (see Fig. 6). Water is fed to the FC through a coaxial tube, also acting as vacuum-tight rod for the FC's pneumatic movements.

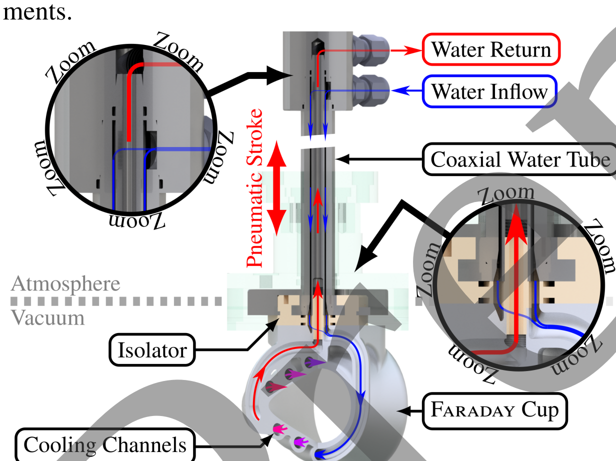

Figure 6: CAD rendering of a sectional view of the FC with a schematic depiction of the cooling water flow.

Beam Screen

To obtain a direct image of the beam's transversal charge distribution, a *Chromox* scintillation screen can be inserted (see Fig. 7). The L-PBF-manufactured screen holder is water-cooled with a meandering cooling channel pattern along the screen's back and replicates the FC's coaxial water flow. The beam image can be monitored using a digital 1/2.5″ CMOS camera with 25 mm magnifying lens. The camera's point of view is shown in Fig. 7 (right). As the image is observed under an angle, maximizing its horizontal size, projection and optical errors have to be considered. Here, the image analysis software of [7] offers error corrections and various analysis capabilities.

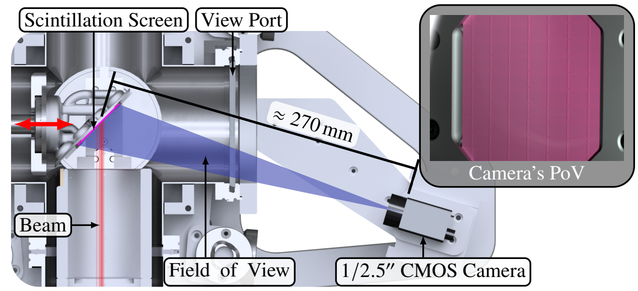

Figure 7: CAD rendering of a sectional view of the pneumatically inserted BS, the camera's geometric field of view and its simulated point of view (PoV, right).

Current Status

CAD design of all major components is finished and all SEM, FC and BS components have been manufactured. FC and BS are fully assembled (see Fig. 8) and leak rate measurements of their cooling systems and pneumatic rods are ongoing. The SEM is expected to be assembled soon, allowing to join all diagnostic components into the section's vacuum chamber.

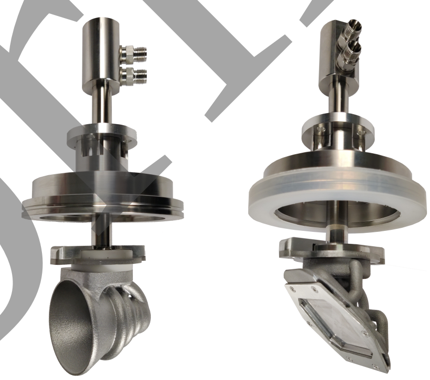

Figure 8: Assembled FC (left) and BS (right).

REFERENCES

[1] "The AEG isochronous cyclotron at the University of Bonn", *IEEE Trans. Nucl. Sci.*, Vol. 13, No. 4, (1966). doi:10.1109/TNS.1966.4324267

[2] D. Sauerland *et al.*, "Status of the Bonn Isochronous Cyclotron", in *Proc. IPAC'24*, Nashville, TN, USA, May 2024, pp. 3539-3541. doi:10.18429/JACoW-IPAC2024-THPR22

[3] D. Sauerland *et al.*, "Proton irradiation site for Si-detectors at the Bonn Isochronous Cyclotron", in *Proc. IPAC'22*, Bangkok, Thailand, Jun. 2024, pp. 130-132. doi:10.18429/JACoW-IPAC2022-MOPOST030

[4] H.P. Beck and R. Langkau, "Die Sekundärelektronen-Ausbeute verschiedener Materialien bei Beschuß mit leichten Ionen hoher Energie," *Zeitschrift für Naturforschung A*, vol. 30, no. 8, pp. 1055–1062, 1975. doi:10.1515/zna-1975-0822

[5] E.F. da Silveira and J.M.F. Jeronymo, "Secondary electron emission from the entrance and exit surfaces of thin aluminium foils under fast light ion bombardment," *Nucl. Instrum. Methods Phys. Res. Sect. B*, vol. 24–25, pp. 534–537, (1987). doi:10.1016/0168-583X(87)90702-6

[6] H. Rothard, K.O. Groeneveld, and J. Kemmler, "Kinetic electron emission from ion penetration of thin foils in relation to the pre-equilibrium of charge distributions," in *Particle Induced Electron Emission II*, Springer Tracts in Modern Physics, vol. 123, Springer-Verlag, Berlin, Heidelberg, 1992, pp. 97–147. doi:10.1007/BFb0038299

[7] M. Switka *et al.*, "Progress on distributed image analysis from digital cameras at ELSA using the RabbitMQ message broker", in *Proc. IBIC'23*, Saskatoon, Canada, Sept. 2023, pp. 449-452. doi:10.18429/JACoW-IBIC2023-WEP046